

Dynamic Nanofragmentation of Carbon Nanotubes

Chiara Daraio, Vitali F. Nesterenko, Joseph F. Aubuchon, and Sungho Jin*

Materials Science and Engineering Program, Mechanical and Aerospace Engineering Department, University of California, San Diego, La Jolla, California 92093-0411

Received July 6, 2004; Revised Manuscript Received August 13, 2004

ABSTRACT

We report a new phenomenon of dynamic nanofragmentation of DC plasma grown carbon nanotubes under high-strain-rate conditions. An impacting sphere on vertically aligned multiwall nanotubes caused them to break up into short segments in just 15 microseconds with a relatively uniform length range of ~ 100 – 150 nm. The ends of the fragmented nanotubes often exhibit an irregular oval or hexagonal cross-section. Some of the fragments show a sign of plastic bending near the fracture point. The mechanisms of multiple-breakup of nanotubes may be tentatively attributed to elastic buckling and fracture at the nodes or weak points, sequential fragmentation due to local bending, or contact interaction of crossed nanotubes. The observed cutting of nanotubes may conveniently be utilized for their resizing and end-opening for a variety of applications such as nanocomposite synthesis, nanoscale and large-surface-area reservoirs to store chemical reactants/catalysts, nanocarriers for therapeutic drugs/DNAs/proteins, and various other nanoelectronics and nanomechanics applications.

Since their discovery, the processing and properties of carbon nanotubes (CNTs) have been investigated for many different technical applications. While the growth of long nanotubes is relatively easy, controlled cutting of nanotubes into desired short lengths has not been studied much. For a number of technical applications, cutting of nanotubes (and nanowires in general) into desired short lengths, preferably of equal or comparable lengths, is essential. For example, nanoelectronics, nanocircuit interconnections, nanooptics (nano laser array), NEMS (nanoelectromechanical systems) devices including nanomanipulators, AFM tips, biomedical applications for interaction with DNAs,^{1,2} sensors, actuators, and so forth require a controlled and manageable length, rather than the often uncontrollably long nanotubes. Some applications require opening of nanotubes especially for filling the inside with other materials or for chemically functionalizing the open ends for advanced composites or for biochemical conjugations. At least one end is usually closed in the as-synthesized nanotubes as the growing nanotube tip is terminated with either a dome or a catalyst particle. Cutting or opening of nanotubes is typically carried out by etching with concentrated acids, such as nitric acid, or by mechanical grinding. However, most of these processes result in uncontrolled cut lengths and often cause structural damage such as amorphization or disrupted nanotube walls.^{3,4} Furthermore, none of these methods allows convenient cutting into nanoscale lengths of 100–200 nm. A cutting/opening technique for producing short, relatively straight CNTs without damaging the structure of nanotubes is therefore

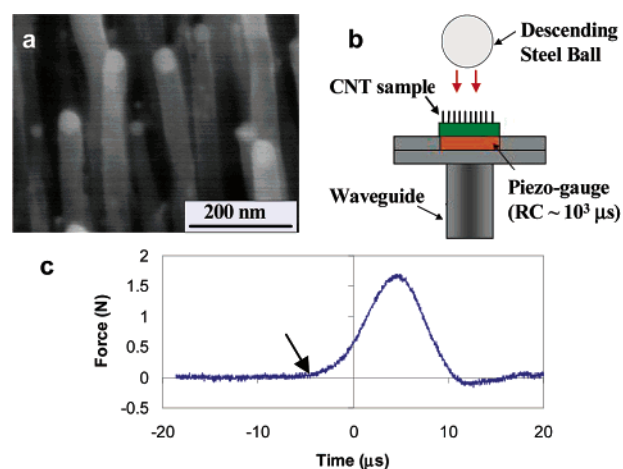


Figure 1. (a) SEM micrograph of the aligned nanotubes. (b) Experimental setup for measurement of dynamic contact force applied to the forest of nanotubes. (c) Force–time curve of the vertical impact on the CNT array.

desirable. In this paper we present a new phenomenon of simple, high-strain-rate, head-on impact cutting the length of carbon nanotubes into a multitude of more or less uniform length pieces with open ends, and we discuss possible mechanisms for such a phenomenon.

Vertically aligned carbon nanotubes have been fabricated by various experimental methods, including DC plasma, microwave, or thermal CVD (chemical vapor deposition) processes.^{5–10} In the present work, arrays of vertically aligned carbon nanotubes (CNTs) were tip-grown, as shown in Figure 1a, using a DC plasma enhanced chemical vapor deposition (PECVD) method. Our array of aligned carbon nanotubes

* Corresponding author. E-mail: jin@ucsd.edu.

was fabricated by first sputtering a ~ 5 nm thick Ni film over the surface of an n-type Si (100) substrate. The substrate was then transferred to the CVD chamber. Upon heating to ~ 700 °C under hydrogen flowing at 150 sccm (standard cubic centimeter per minute) and held at 15 Torr, the Ni film breaks into islands with average diameters ~ 40 nm, which serve as nanotube nucleating islands. The atmosphere was changed to ammonia (NH_3) flowing at 150 sccm and held at 3 Torr, and a DC bias of 450 V was applied between the anode above the sample and a cathode which supports the sample. Under the applied voltage, plasma was formed and acetylene (C_2H_2) gas was then added to the chamber flowing at a rate of ~ 30 sccm with the total NH_3 and C_2H_2 pressure held at 3 Torr. After ~ 30 min of CVD processing, vertically well aligned multiwall nanotubes (MWNTs) were formed. The SEM (scanning electron microscopy) analysis was carried out using a Philips field emission SEM operated at 30 kV.

The arrays had a density of $\sim 2 \times 10^9$ CNTs/cm². The average length of the nanotubes was ~ 1.5 μm . The SEM micrograph also showed a well-defined tip growth mechanism with the Ni catalyst particles always present at the tip of growing nanotubes. The experimental setup used here for high strain rate deformation consisted of a benchtop system¹¹ (see Figure 1b) which included a free-falling sphere (precision chrome steel ball bearing grade 25, diameter 2 mm, surface roughness (RA) ~ 50 nm maximum, made from AISI type 52100 steel, McMaster-Carr cat.) and a calibrated piezosensor connected to a Tektronix oscilloscope to detect force–time curves to help control the overall dynamic force applied to the forest of CNTs. The use of a sphere allows a reproducible application of large, concentrated force so that each nanotube can be subjected to sufficient impact energy. A steel shock-absorbing rod structure (waveguide) was placed under the sensor to avoid possibly reflecting waves from the support bench.

The impact on the aligned nanotubes was generated by dropping the 2 mm diameter steel sphere (0.03 g weight) from a height of 2 mm, which corresponds to a speed of impact of ~ 0.2 m/s. Accordingly, the overall strain rate is calculated to be on the order of 10^4 – 10^5 s⁻¹. Shown in Figure 1c is a force–time curve for the vertical impact of the descending metal sphere on the nanotube array measured by the set up of Figure 1b. The duration of the impact pulse is ~ 15 μs and the average maximum force applied on the overall sphere-forest of the nanotube contact area is ~ 1.7 Newton, which corresponds to a force of $\sim 4.3 \times 10^{-5}$ N/per single CNT. The ball displacement, starting from the point of contact with nanotubes (shown by the arrow c) until it comes in contact with the layer of fragmented nanotubes at the bottom, is estimated to be ~ 1.0 μm , comparable to the average height of the CNTs. The maximum pressure exerted on the impacted area, estimated from the force and the sphere–nanotube contact area (~ 50 μm in diameter central portion of the contact area), is very high, amounting to ~ 8.7 kbar (0.87 GPa).

The energy used for deformation and fracture of nanotubes derived from the initial kinetic energy of the ball and the

calculated coefficient of restitution ($e = 0.6$) based on experimental data is 0.36 μJ (5.8×10^{-26} eV). Assuming that this energy is uniformly distributed among the CNTs in the impacted area, we can derive a localized energy per nanotube of 9.2×10^{-6} μJ (1.5×10^{-30} eV/CNT). This amount of energy is well below the energy necessary to break C–C bonds in the nanotube (C–C binding energy is known to be ~ 7.4 eV/atom, which is many orders of magnitude larger than the energy supplied here). A possible explanation of the fragmentation phenomena observed at such a low energy level may be due to the inclined graphene walls (herringbone geometry) with respect to the nanotube axis in the DC plasma CVD grown nanotubes.⁸ In this case we may expect breaking of the weaker bonds between graphene layers instead of breaking the strong C–C bonds in the graphene sheet. To test this hypothesis, we prepared vertically aligned arrays of multiwall carbon nanotubes with graphene walls parallel to the nanotube axis using a microwave plasma CVD system.⁹ With such nonherringbone type nanotubes, we were unable to fracture the nanotubes on identical vertical sphere impact conditions, which implies that the observed nanofragmentation in the DC plasma nanotubes occurs via low-energy separation between inclined graphene sheets.

The impact experiments of Figure 1b were also carried out for different nanotube lengths (1–3 μm) and impact velocities in the range of 0.1–0.5 m/s; similar mechanical behavior and fragmentation phenomena were observed.

It is seen that the aligned nanotubes of Figure 1a are broken into many segments (Figure 2) with relatively comparable lengths of ~ 100 – 150 nm on average (although occasional variation of length outside this range is observed). The observed fragmented length is a few times larger than the maximum surface roughness (RA) of the ball (~ 50 nm); the correlation between the surface roughness and the final size of the fragments might be an interesting topic for future studies. For the ~ 1.5 μm tall nanotubes, this means a fragmentation of each nanotube into ~ 10 – 15 segments. As the average diameter is ~ 40 nm and the nano fragmented length is ~ 100 – 150 nm, the aspect ratio (the length-to-diameter ratio) of each of the short nanotubes is only about 3. This short aspect ratio implies a relatively convenient and easy penetration/incorporation of another material inside these open nanotubes, for example, to prepare new types of nanocomposite materials with unique mechanical, magnetic, electronic, or optical properties. These nanolength, hollow CNTs can also be utilized as a nanoscale and large-surface-area reservoir to store chemical reactants/catalysts or therapeutic drugs/DNAs/proteins to be delivered. The observed phenomenon of nanoscale fragmentation with such a relatively uniform length-distribution is very interesting, as one would normally expect to see a rather random length-distribution of fractured segments. Such a phenomenon, to the best of our knowledge, has not been reported so far. The open ends of the nanofragmented CNTs often exhibit slightly distorted or oval shaped openings as shown in Figure 2a and b, which was obviously caused by the deformation and fracture process. A relatively well-defined hexagon shaped opening was also observed, an example of which is marked

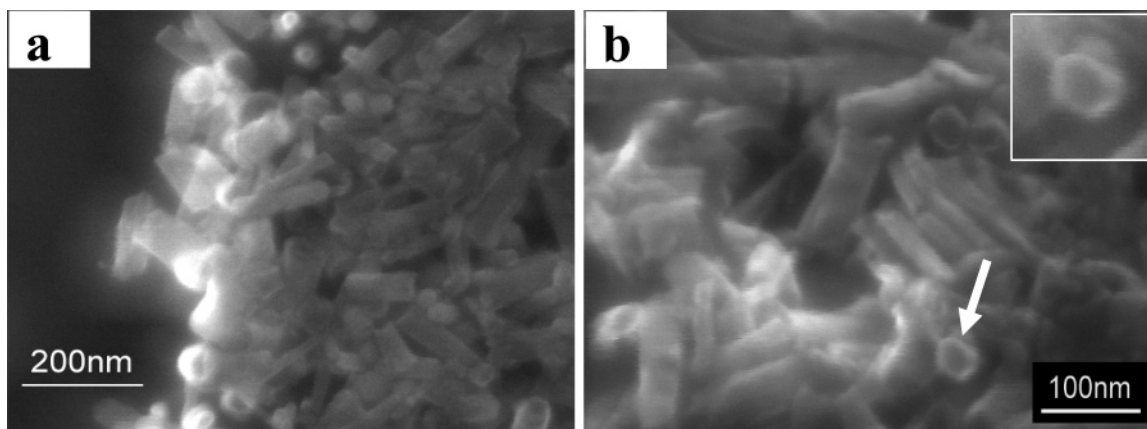


Figure 2. Two examples of nanofragmented carbon nanotubes (a) lower magnification, (b) higher magnification showing hexagonal or oval cross-section openings formed by impact deformation.

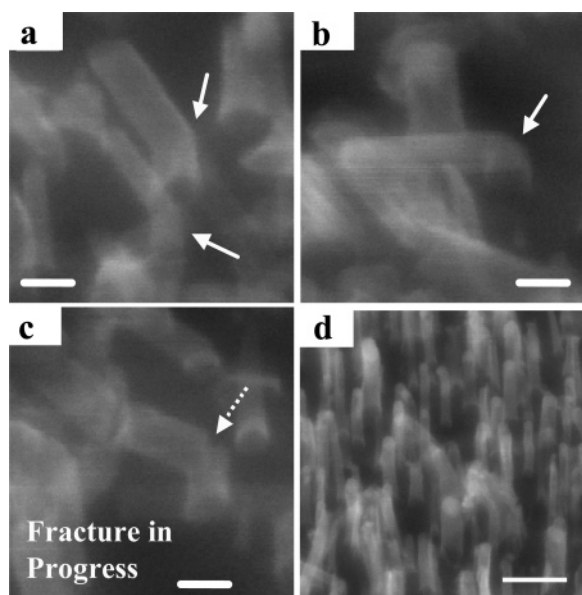


Figure 3. Carbon nanotubes after impact deformation showing local plastic bending (see arrows in (a), (b)) and the onset of fracture (dotted arrow in (c)). The plastic deformation is obvious in the curved sections near some of the fragmented ends of the nanotubes. (d) SEM micrograph showing short remnant nanotubes in the off-centered region after impact fragmentation. Scale bars for (a)–(c) are 50 nm, (d) 200 nm.

by an arrow and inset in Figure 2b. The occurrence of a hexagon-shaped nanotube cross section was predicted by Chesnokov et al. on elastic compaction of nanotubes bundles.¹² Whether our observation of fractured and permanently hexagon- or oval-shaped nanotube ends is related to the Chesnokov prediction is unknown. The noncircular shape of the openings in some of the nanofragmented nanotubes as compared to the originally circular cross-section of as-grown carbon nanotubes implies their plastic deformation during impact. Such plastic deformation is also evident from Figure 3 (a–c) which shows curved sections near the fragmented ends of the nanotubes. The plastic deformation most likely involves an introduction of crystallographic defects, such as the formation of the well-known pentagon and heptagon defects or Stone–Wales pairs (5-7-7-5 defects)

on the normally hexagonally shaped arrangement of carbon atoms on graphene planes of the carbon nanotubes. Partial fracture of the CNT or bent tubes still partially attached to the remaining vertical segments (about 100–200 nm tall) still standing on the substrate were observed in the slightly off-centered region where the curvature of the sphere prevented it from touching the surface of the substrate (Figure 3d). Further study of plastic deformation and fracture behavior of carbon nanotubes on head-on impact might be an interesting area for in-depth research, especially the bending/breaking mechanisms associated with impact deformation.

From the geometry of the 2 mm diameter metal sphere descending and penetrating through the thickness of the carbon nanotube array ($\sim 1.5 \mu\text{m}$ tall), the sphere–nanotube contact area is estimated to be $\sim 90 \mu\text{m}$ in diameter. Of this contact area, the central region of impact with a diameter of roughly $\sim 50 \mu\text{m}$ shows essentially completely fractured nanotubes in segments of 100–150 nm lengths. In this region, the bottom surface of the 2 mm diameter descending sphere is practically flat, with the contact angle between the nanotube tip and the bottom surface of the ball is between 0 and 1.15° . In the noticeably off-centered region just outside this $\sim 50 \mu\text{m}$ diameter, e.g., an area forming a $\sim 20 \mu\text{m}$ wide ring around the central part of the impact, most of the nanotubes are also fractured into nanofragments. The short, bottom sections of nanotubes though are still attached to the substrate. This is because the portion of the sphere contacting this off-center area is tilted and cannot touch the substrate. Such remnant sections of nanotubes with a height of ~ 100 – 200 nm are shown in Figure 3d. Carbon nanotubes are known to have superior mechanical properties;¹³ for example, a forest of CNTs grown in a microwave plasma system did not break under similar conditions of impact and can be exploited for strongly nonlinear springs.¹¹ Mechanisms of fracture and axial and radial deformation of carbon nanotubes have been studied extensively with the aid of theoretical calculations and some in-situ analysis.^{11,13–15} However, there has been no report on the head-on impact fragmentation behavior of carbon nanotubes such as being described in this work.

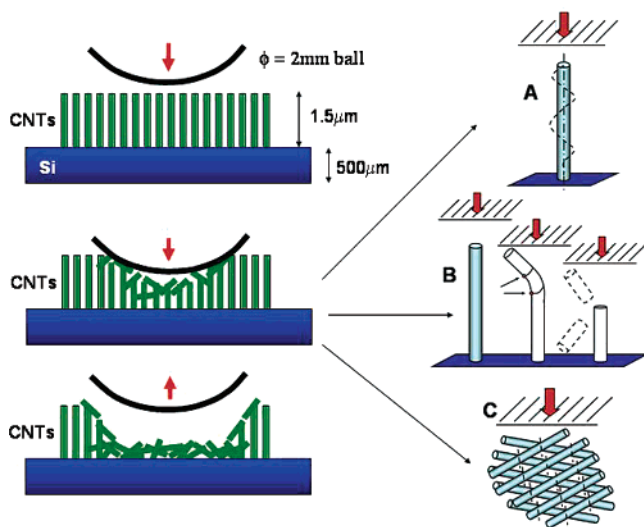


Figure 4. Initial, intermediate, and final stages of impact are shown on the left portion of the figure. On the right, possible fragmentation mechanisms suggested: (A) buckling, (B) sequential fragmentation, (C) fracturing of crossed net nanotubes, and/or a combination of any of the above.

Initial, intermediate and final stages of impact and possible mechanisms considered for the observed nanofragmentation are illustrated schematically in Figure 4 and are discussed as follows. (A) The ball impact on vertically aligned nanotube generates a critical compression stress resulting in the elastic buckling of the nanotube, which may be considered as an elastic column fixed at the base and free at the side of impact (Euler instability¹⁶). The theory allows an infinite number of buckled mode shapes (defined by integer n) depending on the applied axial force. In the case of quasi-static loading of single isolated column, the only mode of practical interest is $n = 1$. In the case of dynamic loading on aligned nanotubes, a higher order buckling mode is possible ($n = 1-20$ in our case). There could be a number of other ways of generating higher order modes, one example being the contact interaction and blocking by neighboring nanotubes. Another alternative is a multiple nucleation of cracks in the first order buckling mode ($n = 1$) and subsequent distributed fracturing originating from all these nucleation sites where stress is exceeding the critical fracture stress. It is conceivable that such multiple nucleation sites can even be purposely introduced during CVD growth via periodic doping, change of deposition parameters, or introduction of lattice or geometrical defects (such as sharp-bending zigzag nanotubes¹⁷). This mechanism may be supported by the observation of rather uniform and short fragment length. (B) Breaking of the nanotubes due to local bending and fracture progressing from the tip to the base in a sequential manner as the sphere continues to descend, which may be supported by observation of remnant, still vertically attached nanotube segments shown in Figure 3d. Surface roughness, being comparable to the diameter of the nanotubes, can be important in establishing boundary conditions on the contact of the nanotubes with the ball surface

(free or clamped), therefore effecting the size of the fragments. (C) Each of the nanotubes in the impact area is first broken into a few long pieces (e.g., due to mechanism A or B), which fall on the substrate surface creating a crossed net of overlapping tubes and then fragmented by vertical compression. While the average mesh size of the net, and the subsequent length of the segments, appears to match the estimated density of nanotubes on the substrate, the formation of such a periodically arranged mesh structure in a short time period of ~ 15 microseconds seems less likely.

Further research is needed to understand the exact mechanism for the observed nanofragmentation of carbon nanotubes. It would be interesting to see if similar nanofragmentation occurs on z -direction impact stressing of other types of aligned nanowires, for example, ZnO, GaN, Si, SiO₂, etc. The observed cutting of nanotubes may conveniently be utilized for resizing and end-opening for easier filling of nanotubes with other materials for synthesis of nanocomposites or nanocarriers of catalysts for chemical reactions, or proteins, DNAs/genes, and drugs for biomedical applications, for easier handling of shortened nanotubes or nanowires for other potential applications such as in nanoelectronics, nanointerconnections, nanomanipulators, sensors, and actuators.

In summary, a new phenomenon of dynamic nanofragmentation of CNTs into short lengths has been observed and analyzed for the first time. This rapid technique may conveniently be utilized for resizing and end-opening nanotubes for a variety of applications.

Acknowledgment. The research support from NSF under Grant No. DCMS03013220 and NSF-NIRT under Grant No. UKRF 4-65998-03-129 is gratefully acknowledged.

References

- (1) Baker, S. E.; Cai, W.; Lasseter, T. L.; Weidkamp, K. P.; Hamers, R. *J. Nano Lett.* **2002**, *2*, 1413.
- (2) Gao, H. J.; Kong, Y.; Cui, D. X.; Ozkan, C. S. *Nano Lett.* **2003**, *3*, 471.
- (3) Jia, Z. J.; Wang, Z. Y.; Liang, J.; Wei, B. Q.; Wu, D. H. *Carbon* **1999**, *37*, 903.
- (4) Monthieux, M.; Smith, B. W.; Burteaux, B.; Claye, A.; Fischer, J. E.; Luzzi, D. E. *Carbon* **2001**, *39*, 1251.
- (5) Rao, A. M. et al. *Appl. Phys. Lett.* **2000**, *76*, 3813.
- (6) Ren, Z. F. et al. *Science* **1998**, *282*, 1105.
- (7) Teo, K. B. K. et al. *Appl. Phys. Lett.* **2001**, *79*, 1534.
- (8) Merkulov, V. I.; Melechko, A. V.; Guillorn, M. A.; Lowndes, D. H.; Simpson, M. L. *Appl. Phys. Lett.* **2001**, *79*, 2970.
- (9) Bower, C.; Zhu, W.; Jin, S. H.; Zhou, O. *Appl. Phys. Lett.* **2000**, *77*, 830.
- (10) Bower, C. et al. *Appl. Phys. Lett.* **2002**, *80*, 3820.
- (11) Daraio, C.; Nesterenko, V. F.; Jin, S., *to be published*.
- (12) Chesnokov, S. A.; Nalimova, V. A.; Rinzler, A. G.; Smalley, R. E. *Phys. Rev. Lett.* **1999**, *82*, 343.
- (13) Pantano, A.; Parks, D. M.; Boyce, M. C. *J. Mech. Phys. Solids* **2004**, *52*, 789.
- (14) Yakobson, B. I.; Brabec, C. J.; Bernholc, J. *Phys. Rev. Lett.* **1996**, *76*, 2511.
- (15) Falvo, M. R. et al. *Nature* **1997**, *389*, 582.
- (16) Gere, J. M.; Timoshenko, S. P. *Mechanics of Materials*, 3rd ed.; PWS-KENT Publishing Company: Boston, **1990**.
- (17) AuBuchon, J. F.; Chen, L.-H.; Gapin, A. I.; Kim, D.-W.; Daraio, C.; Jin, S. *Nano Lett.* in press.

NL048946K